Volc. Seis., 2000, Vol. 21, pp. 443-463
Reprints available directly from the publisher
Photocopying permitted by license only

Modeling the Intensity–Magnitude–Distance Relation Based on the Concept of an Incoherent Extended Earthquake Source

A. A. GUSEV* and L. S. SHUMILINA**

* *Institute of Volcanic Geology and Geochemistry, Far East Division, Russian Academy of Sciences, Petropavlovsk-Kamchatsky, 683006 Russia*

** *United Institute of Physics of the Earth, Russian Academy of Sciences, Moscow, 123810 Russia*

(Received February 1, 1999)

Parameters of short period motion radiated by earthquake sources were modeled to provide a theoretical description of macroseismic patterns. The energy contributions due to the radiating elements, source components that generate the field recorded by the receiver, were assumed to be additive. It is suggested that the integral of the square of accelerograms or the "Arias intensity" can be used as a parameter suitable for predicting intensities (a modification of an approach developed by F. F. Aptikaev and N. V. Shebalin). The source of an earthquake is assigned a moment magnitude. Sources are assumed to obey geometrical similarity. The theory and empirical data are compared for two regions: Kamchatka–Kurils–Japan and continental North Eurasia. The far-field intensity vs. moment magnitude relation is practically linear and points to the growth of amplitude acceleration spectrum in accordance with the squared-omega-model or slightly faster. The method proposed here was employed to predict intensity in the two regions as a function of magnitude and distance using the extended source model.

INTRODUCTION

The use of contemporary and historical macroseismic data (usually given as observed intensities) is an important tool for the analysis and prediction of earthquake hazard. Until now seismologists relied on empirical relations alone for analyzing intensity maps and deriving intensity–magnitude–distance relations. This creates difficulties in the way of

solving practical problems such as extrapolation of moderate amplitude data to large amplitudes, the transfer of known empirical relations for use in new regions, and integrated analysis of macroseismic and instrumental observations.

Now the intensity–magnitude–distance relationship (I–M–r) can be analyzed on a theoretical basis using the short-period radiation of an extended source. In the first place, recent models of short period earthquake source radiation [4], [28] provide a realistic average description of the wave field around the source in terms of the field amplitude parameters. Secondly, there is a better understanding of a relation between macroseismic intensity I and wave-field parameters. Gutenberg and Richter [20], Kanai [25], and many other workers on the lines of these pioneers compared intensity to peak acceleration $a_{\max}$ or to the peak velocity $V_{\max}$ of ground motion. New prospects are offered now by integral ground motion parameters such as the combination $a^2_{\max}d$ [1], [2], where d is ground-motion duration, or another similar parameter, the maximum ordinate of acceleration Fourier spectrum $F_{\max}$ [14]. These parameters incorporate ground motion duration, which is necessary to account for the fact that the actually observed damage to buildings and engineering structures is greater for longer durations of ground motion at a constant amplitude. The modeling of the $I(\mathrm{M}, r)$ relation based on wave field parameters will presumably provide a better description and prediction of intensities than is possible on a purely empirical basis.

The model of the wave field near an incoherent source and the $I(a_{\max}, d)$ relation were first combined by Gusev [4], who derived a first theoretically sound $I(\mathrm{M}, r)$ relation. Earlier Evernden [21] suggested the use of a semiempirical model for an extended macroseismic source treated as a sequence of point sources. Here we develop this approach further. Departing from the crude source model [4] represented by a disc of constant radiation intensity, we use a somewhat more realistic model of a rectangular source. For this source we derive models of isoseismals and, based on these, a relation of intensity I versus moment magnitude M_W and distance r.

The use of the seismic moment M_0 or moment magnitude M_W as an integral measure of earthquake source power instead of ordinary magnitudes is an important part of our approach. It is this circumstance that can hopefully provide a reliable extrapolation of empirical data represented by the $I(\mathrm{M}_W, r)$ relation to extremely large magnitudes.

Empirical data of two kinds are used here to find the model parameters:

$$I(\mathrm{M_W}, r)\big|_{r=100} = I_{100}(\mathrm{M_W}),$$
$$I(\mathrm{M_W}, r)\big|_{\mathrm{M_W=const}} = I(r).$$

The result is a new scheme of calculation suitable for the practical prediction of intensities and modeling the near-field isoseismals. By eliminating the difficulties inherent in the existing methods, this new approach enables one to take into account the fact that the intensity of shaking is saturated near an extended source, avoid potential errors due

to the internal nonlinearity and saturation of intensity scales, and obviate the problem of choice between the Covesligetti and the Blake-Shebalin formulas [15].

The model proposed here was developed and tested in two seismic regions of Russia.

GENERAL PRINCIPLES OF MODELING INTENSITIES BASED ON PHYSICAL PARAMETERS OF GROUND MOTION

The first requirement for a practical modeling of intensities is to find a specific relation connecting intensity and physical parameters of ground motion. Gutenberg and Richter [20] put forward the relation

$$I = 3\lg a_{max} + \text{const}, \tag{1}$$

where a_{max} is peak ground motion acceleration. Shebalin [16] summarized data from the literature to corroborate (1) as an average relation accompanied by a large data scatter. This relation was repeatedly revised. Medvedev [8] and Shebalin [16] proposed the form

$$I = 3.3\lg a_{max} + \text{const}. \tag{2}$$

to serve as a standard for the most important intensity range of V to VIII. Also, Shebalin [16] remarked that the $I(a_{max})$ relation was actually nonlinear. Based on a sequence of preliminary studies, Aptikaev and Shebalin [2] proposed a relation of the form

$$I = f(\lg a_{max} + 0.5\lg d_A) + \text{const}, \tag{3}$$

where d_A is the duration defined by F. F. Aptikaev as the length of that part of the accelerogram where amplitudes are above 50% of the maximum. The function f was specified in tabular form and expressed the nonlinearity referred to above; for the range I = VI–IX it is close to

$$I = 3.33\lg(a_{max} d_A^{0.5}) + \text{const}. \tag{4}$$

Kanai [25] suggested a relation to be sought between intensity and peak ground velocity V_{max}. Medvedev [8] recommended the relation

$$I = 3.33\lg V_{max} + \text{const}. \tag{5}$$

Chernov [14] noted a close relation of intensity to the maximum of acceleration spectrum F_{max}. Housner [24] suggested relating I to the area under the plot of velocity response spectrum.

The approaches advocated by F. F. Aptikaev, N. V. Shebalin, Yu. K. Chernov, and in part by G. Housner, all pivot on the use of an integral characteristic of ground motion instead of a peak value; this is consistent with what is observed in the destruction of buildings. The simplest integral characteristic is the integral of the square of ground acceleration:

$$A = \int a^2(t)dt, \tag{6}$$

where $a(t)$ is an accelerogram. The quantity A was called the "Arias intensity". Denoting

$$A_{AS} = a^2_{max} d_A \tag{7}$$

we notice that Arias' A and Aptikaev–Shebalin's A_{AS} are similar in physical meaning. Besides, $A \approx F^2_{max}/2\Delta f$, where Δf is an effective frequency width which can to a first approximation be treated as constant. The basic quantity for this study will be A. Unfortunately, the relation between A and I was not examined. For our derivation of empirical formulas we assume this relation to be linear and close to the A_{AS}–I relation. Now using (4) we get

$$I = C_A \lg A + \text{const}. \tag{8}$$

Using the usual relation $\partial \lg a_{max}/\partial I = \lg 2$, we put $C_A = 1.667$ in accordance with (4). The method of calculation used below enables some small deviations of C_A from the adopted value to be corrected.

We now describe how the A field around a source can be found. Following [4], we assume the source to be an area whose elements emit high-frequency (short-period) radiation independently of one another (incoherently). That means that the contributions due to different component areas are summed at a receiver in energy (the total instantaneous power equals the sum of the instantaneous powers which are the contributions due to elementary sources, the same being true of the energies). For the case in hand this means that, at a receiving site, one has

$$a^2(t) = \sum_{i=1}^{N} a_i^2(t), \tag{9}$$

$$A = \sum_{i=1}^{N} A_i, \tag{10}$$

where $a_i(t)$ and $A_i = \int a_i^2(t)$ are the accelerogram and the contribution into A which are due to elementary source i ($i = 1, 2, 3, \ldots, N$). To find A_i, we first define a standard function $\Phi(r)$ governing the attenuation of the Arias intensity due to a point source as follows:

$$A(r) = A(r_0)\Phi(r)/\Phi(r_0), \tag{11}$$

where r_0 is a standard distance. We put $r_0 = 1$ and $\Phi(r_0) = 1$ for simplicity. The elementary source is assumed to be small and isotropic, so that

$$A_i = E_i \Phi(r_i), \tag{12}$$

where r_i is the source–receiver distance and E_i the "energy" of an elementary source, defined as the A_i for unit distance.

It can be supposed that the main contribution into ground motion is due to S waves whose radiation pattern (for the square of the acceleration vector length) is centrally symmetric and does not contain any nodal lines. This pattern is close to spherical, because the source anisotropy due to the radiation pattern is almost never seen in the isoseismals. For this reason we thought it possible to use the model of an isotropic elementary source.

When the attenuation function $\Phi(r)$ is known and the positions of elementary sources with some E_i are specified, then relations (8), (10) and (12) can be used to deal with practical problems arising in calculation of intensities. One can adjust theoretical isoseismal maps for specified sources, actually solving the inverse problem of radiator structure by the trial-and-error method or examine the average $I(M_W, r)$ relation by calculating intensity fields for simple source geometries, the magnitude being varied as a parameter. The second procedure will be discussed below. Before coming to the scheme of calculation, we discuss the choice of $\Phi(r)$.

It can be seen from maps of actually observed isoseismals that the very description of attenuation in terms of a distance function is oversimplified and is unable to explain the often rather complicated structure of these maps. However, this approach can be considered acceptable for the restricted purposes of the present study. The well-known intensity attenuation laws due to Blake-Shebalin and Covesligetti [15]

$$I(r) = \Phi_1(M) - C\lg r, \tag{13a}$$

$$I(r) = \Phi_2(M) - C\lg r - qr, \tag{13b}$$

the latter being a generalization of the former, suggest a slightly modified conventional attenuation model

$$\Phi(r) = r^{-2n}\exp(-r/r_Q) \equiv g(r,n,r_Q). \tag{14}$$

With the right choice of the exponent n and a narrowband accelerogram (the mean frequency is f_1) one has

$$r_Q = cQ(f_1)/2\pi f_1, \tag{15}$$

where c is S-wave velocity and Q is an S-wave Q-factor. When $Q(f_1) = Q_0 f^1$, which is often a realistic assumption, then r_Q (the distance over which the "energy" is attenuated by a factor of e, see (15)) is independent of the frequency, so relation (15) is valid even for a broadband acceleration spectrum.

When neither of the above variants works, and when the parameter n or the coefficient C_A were chosen wrongfully, the estimation of r_Q from observations no longer has a direct bearing on the shear-wave Q-factor, becoming merely a fitted constant.

A more complex attenuation model may arise in some regions, consisting of two branches with different n and r_Q:

$$\Phi(r) = \begin{cases} g(r, n_1, r_{Q1}) \text{ for } r < r_C; \\ c_g g(r, n_2, r_{Q2}) \text{ for } r > r_C, \end{cases} \tag{14a}$$

where $c_g = g(r_C, n_1, r_{Q1})/g(r_C, n_2, r_{Q2})$; r_C is the distance at which the attenuation law is switched from the first branch with parameters n_1, r_{Q1} to the second with n_2, r_{Q2}.

CALCULATION OF THE MEAN I (M_W, r) RELATION

This relation was modeled on the basis of the simplest source concept (Fig. 1), assuming it to be a rectangle with length $L = L(M_W)$ and width $W = W(M_W)$. The "luminosity" of the source was assumed to be constant within the source area; that means that the energy E_i is proportional to the area S_i of the elementary radiator i:

$$E_i = C_S S_i. \tag{16}$$

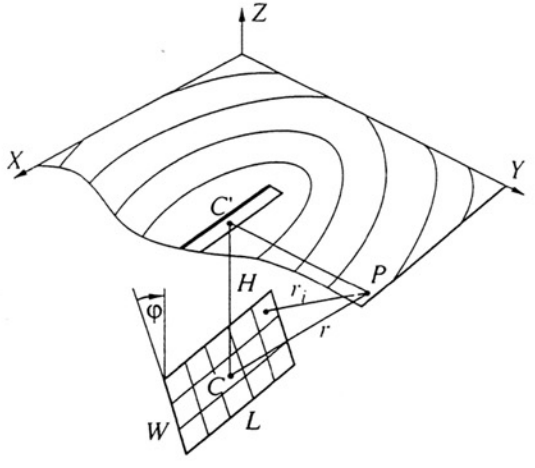

Figure 1 Scheme for intensity calculations: C – hypocenter, C' – epicenter of a rectangular source L long and W wide at depth H dipping at angle φ; the XY plane is the ground surface; P is observation site ("receiver"); r is hypocentral distance; r_i is the distance to i-th subsource; the rectangle on the XY plane is the projection of the source onto the ground surface, the bold side showing the projection of the top of the source; curves on the XY plane are isoseismals due to this source.

Theoretical elementary radiators were obtained using a rectangular grid made by dividing L and W into N_L and N_W identical segments; the total number of radiators was then $N = N_L N_W$, and all S_i were identical:

$$S_i = S/N, \tag{17}$$

where $S = LW$.

Gusev [4] hypothesized that the mean flux of short period power $P = \partial\varepsilon/\partial S\partial t$ (ε being the short period seismic energy of the source) was constant for earthquakes of different magnitudes. If P_M is constant, we assume geometrical and kinematic similarity

$$L \sim W \sim T \sim M_0^{1/3} \sim 10^{0.5M_w} \tag{18}$$

(T is the rupture time) and put $E = \sum E_i \sim \varepsilon$; we then have

$$E \sim \varepsilon = P_M LWT \sim M_0 \sim 10^{1.5M_w}. \tag{19}$$

Hence, using (12), (10), and (8) successively, we obtain for the far zone:

$$I = C_M M_W + \text{const} \tag{20}$$

with $C_M = 2.5$, which is obviously in contradiction with the conventional empirical relation $I = 1.5M_{LH}+\text{const}$, since $\partial M_{LH}/\partial M_W \approx 1$. This implausible result along with some other arguments (see [5]), makes one to reject the idea of a constant P_M.

There is another hypothesis that looks more likely at present, namely, that the specific (per unit area) short period energy density $P_\varepsilon = \partial\varepsilon/\partial S$ of the source radiated by a small area of the source plane during the entire rupture time is independent on the average of how large the source is, which contains this small area (independent of the magnitude).

The hypothesis of constant energy density instead of (19) gives

$$E \sim \varepsilon = P_\varepsilon LW \sim M_0^{2/3} \sim 10^{M_w} \tag{21}$$

and $C_M = 1.667$ in (20); this is quite acceptable.

In virtue of the assumption $F^2_{max} \sim A \sim E$, relation (21) also gives (for the far zone)

$$F_{max} \sim a(f) \sim M_0^{1/3}, \tag{22}$$

which is consistent with the properties of the well-known Aki-Brune ω^{-2}-model [18]. We also note that this basic assumption of numerical similarity between A (6) and A_{AS} (7) neglects the fact that A_{AS} involves a peak rather than an rms acceleration. Analysis shows that for this reason the empirical C_M should be expected to differ from the estimate based on (21), slightly exceeding it; therefore, C_M should preferably be found empirically (see below).

In accordance with the similarity hypothesis (18), we put

$$M_W = \lg S + C_{MS}. \tag{23}$$

Here, $C_{MS} = 4.1$, S being in km^2. The value of C_{MS} is borrowed from [6] where it was based on data available in the literature, [26] in the first place.

To sum up, specifying M_W or S for a source and using (16) one could find the E_i; then A_i via (12) from E_i; then, A via (10) from A_i; and finally, I via (8) from A. However, one

must first determine the numerical values of the constants in (8) and (16). This can be done by calculating the parameters of the radiation field based on realistic source spectra and propagation paths, the final step being to use the $I(a_{\max}, d)$ relation tabulated by Aptikaev and Shebalin [2]. The procedure is rigorous, but very cumbersome. For the time being we circumvented these calculations by calibrating (8) and (16) based on a basic empirical intensity I_b corresponding to a fixed basic combination $(M_W, r) = (M_b, r_b)$.

We now are going to demonstrate that I can indeed be determined, and derive the relevant formulas. Suppose a combination (M_b, r_b) is specified and the value $I_b = I(M_b, r_b)$ is known; also, L and W of the source and its spatial position are given (see Fig. 1). It is required to find I at some "receiver" site (P in Fig. 1). The value of r will be found as a distance between the site and the center of the source. We find $S = LW$ and the areas of elementary radiators using (17). The magnitude M_b is used to find the area of the basic source S_b using (23). Specifying a reasonable ratio of length to width for the basic source, we can determine the source dimensions L_b and W_b.

The relation between I and I_b is more conveniently found, when one is dealing with the far zone for the time being. Take some large $r' \gg L$; $r' \gg L_b$; then all r_i are approximately equal to r'. The values of $I = I'$ and $A = A'$ at distance r' are functions of M_W only. Let us imagine the unknown I' to be fixed and express $I = I(r)$ in terms of $I' = I'(r)$. In virtue of the isotropy assumption I' does not depend on the ray chosen.

For the field of elementary radiator i at distance r', we derive from (10) and (8), assuming the relation $C_A = \partial I/\partial A$ to be valid,

$$A'_i = A'/N, \tag{24}$$

$$I'_i = C_A \lg[(1/N) \times 10^{I'/CA}] = I' - C_A \lg N. \tag{25}$$

The field of the same elementary radiator at distance r_i has the form

$$A_i = A'_i \Phi(r_i/\Phi(r'), \tag{26}$$

$$I_i = I' - C_A \lg N + C_A \lg(\Phi(r_i)/\Phi(r')). \tag{27}$$

Summing the effects due to all elementary radiators at the receiver site, we get

$$A = \sum A_i = \sum A'_i \Phi(r_i)/\Phi(r'), \tag{28}$$

$$I = C_A \lg \sum 10^{I'/CA} = I' + C_A \left\{ \lg \left[(1/N) \sum_i^N \Phi(r_i) \right] - \lg \Phi(r') \right\}. \tag{29}$$

An exactly similar procedure yields the relation of I_b to intensity I'_b at distance r' for the basic earthquake by partitioning the source of the basic earthquake into K elementary radiators:

$$I_b = = I'_b + C_A \left\{ \lg \left[(1/K) \sum_j^K \Phi(r_{bj}) \right] - \lg \Phi(r') \right\}. \tag{30}$$

where r_{bj} is the distance from the receiver to elementary radiator j in the basic source. The receiver is assumed to lie on some (basic) ray at distance r_b from the center of the basic source, the basic ray pointing along the normal to the source plane.

In order to relate I' to I'_b we assume, in accordance with (20), the existence of a relation of the form

$$I' = I'_b + C_M(M_W - M_b), \tag{31}$$

with the C_M not very different from 1.67.

Combining (29), (30) and (31), we get

$$I = I_b + C_M(M_W - M_b) + C_A \left\{ \lg \left[(1/N) \sum_i^N \Phi(r_i) \right] - \lg \left[(1/K) \sum_j^K \Phi(r_j) \right] \right\}. \tag{32}$$

We have ultimately arrived at the master formula to calculate intensity I at a site distant r from the center of a rectangular $L \times W$ source.

It is advisable to consider a slightly more general case, namely, elementary radiators (er) with variable energy ("luminosity"). The luminosity of an elementary radiator can be conveniently described in terms of the effective (ef) area:

$$S_{ef,i} = p_i S_{er}, \tag{33}$$

where p_i is a weight (so far all weights were equal to unity). The matrix p_i specifies the luminosity distribution over the source area. One can see that for (32) to remain valid in the general case, it is sufficient to replace $\lg(1/N) \sum \Phi(r_i)$ with $\lg(\sum p_i \Phi(r_i) / \sum p_i)$ in it. The magnitude M_W of such a source could be defined as

$$M_W = \lg \sum S_{ef,i} + C_{MS}, \tag{34}$$

where M_W is the "macroseismic magnitude" which has no longer to be equal or close to the true moment magnitude, because the proportionality assumption (16) has been dropped.

Formula (32) can be used with the receiver taken at various sites on the ground surface to find I at the sites and plot a map of isoseismals; choosing one or several characteristic rays, one can derive the $I(M_W, r)$ relation. There is good reason to vary the L/W ratio for different M_W. Further, L/W was gradually varied from unity (at $M_W \leq 5$) to three (at $M_W = 9$).

The description of an inhomogeneous source structure in terms of p_i makes it possible to deal with forward and, later, inverse problems for the first one or two isoseismals. For the lower isoseismals one cannot hope to model actual maps by specifying the attenuation

as $\Phi(r)$; a 3-D attenuation structure should be used. These possibilities were not explored in the present study.

Figure 2 presents an example where a map of isoseismals was obtained using the above algorithm for a rectangular source of $L = 155$ km and $W = 52$ km dipping at 30° relative to the vertical; its center was at 40-km depth, the longer axis was horizontal, and the number of subsources was 61×21. The other parameters were as follows: $C_A = 1.667$, $C_M = 1.85$, the attenuation obeys (14) with $n = 1$ and $r_Q = 90$ km, $I_b(M_W = 8, r_b = 100 \text{ km}) = 7.75$ intensity units.

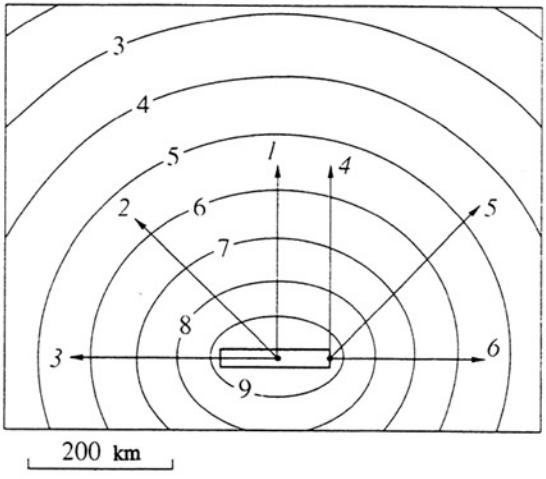

Figure 2 Map of modeled isoseismals due to a $M_W = 8.0$ source at 40 km depth. Arrows show lines 1 through 6.

Figure 3 shows intensity as a function of distance along several differently oriented lines specified in Fig. 2. Also, we determined the intensity as a function of the radius of a circular isoseismal that encloses the same area as does the observed one, this being the usual procedure when dealing with intensity maps. It turned out that the resulting curve was very similar to that along line 2, which had passed through the source center at an angle of 45° to the source axis.

It is important to choose the right interval for the grid of elementary radiators. Distortions are likely to arise with an excessively large interval (Fig. 4). As a matter of fact, the interval should be slightly shorter than the distance between the source and the closest site on the line. Besides, the method of calculation itself relies on the idea of incoherent radiation, but this becomes unjustified at source-receiver distances of the order of the wavelength [4], [5]. Consequently, we did not deal with distances below 5 km.

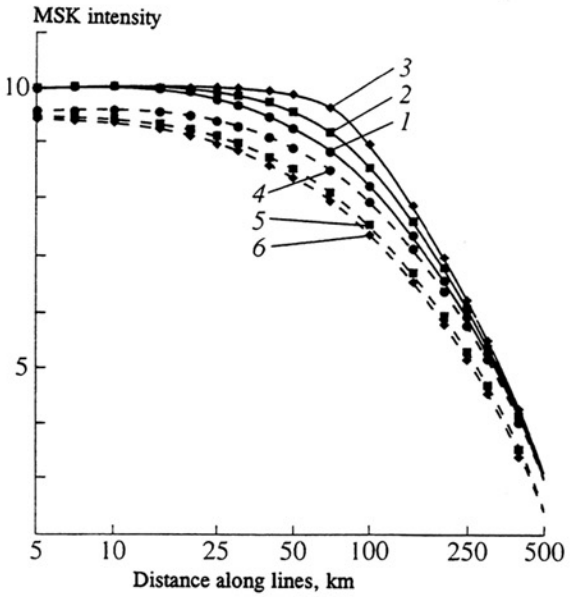

Figure 3 Curves of intensity versus distance along seismic lines (see Fig. 2). Numerals at the curves refer to the lines in Fig. 2.

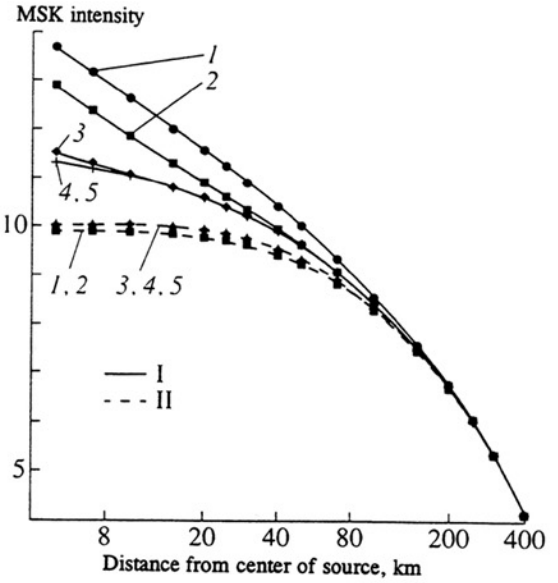

Figure 4 Intensity vs. distance in relation to the number of subsources. Line *1* is as in Fig. 2; I – source at depth 0 km, II – at 40 km. Number of subsources: *1* – 1×1; *2* – 3×1; *3* – 11×3; *4* – 21×7; *5* – 61×21.

DETERMINATION OF EMPIRICAL I (M_W, r) RELATION AND OF PARAMETERS INVOLVED IN THE THEORETICAL (I–M–r) LAW FOR THE KAMCHATKA–KURILS–JAPAN REGION

The approach developed here was tested by deriving $I(M, r)$ for the Kamchatka–Kuril–Japan region. The region was assumed to be homogeneous as to the properties under investigation. We began by testing the linear relation, assumed in (20), between the far-zone intensity of shaking and M_W and finding the coefficient in that relation. To do this we used the Kawasumi method [27] to compare M_W and I_{100}, the intensity at a fixed distance (100 km from the source). Having thus found the $I(M_W)$ relation, independent data were used to determine the $I(r)$ function.

Our determination of $I_{100}(M_W)$ based on Kamchatka and Kuril seismicity (see Table 1) is summarized in Fig. 5. This determination was mainly based on the $r(I)$ for individual earthquakes [9]; where no intensity had been recorded at 100 km distance, the relevant value was interpolated or extrapolated from closest-lying ones (within 20 km). It should be noted that, even when intensities are satisfactorily known on the coast, the I_{100} of many large earthquakes cannot be found with certainty owing to unreliable epicentral coordinates and the resulting uncertainty in the distance.

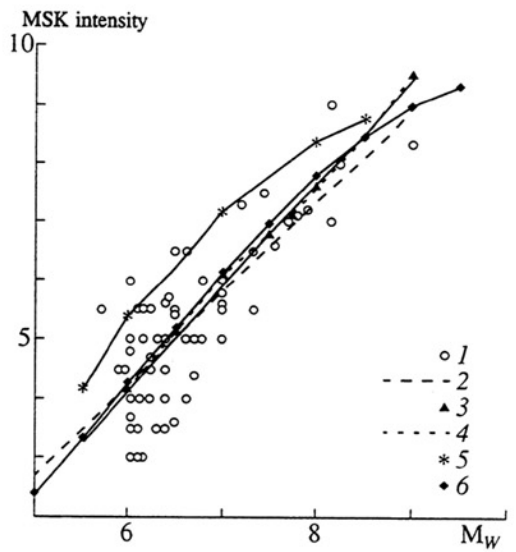

Figure 5 Intensity vs. M_W at 100-km distance for the Kurils, Kamchatka, and Japan: *1* – data points; *2* – linear regression; *3* – orthogonal regression for data points shown; *4* – Hashida relation for Japan [22], [23]; *5* – curve for Kamchatka [13]; *6* – recommended $I_{100}(M_W)$ relation.

Table 1 Earthquakes used to determine I_{100}.

Date (month, year	Magnitude			Date (month, year	Magnitude		
	M_{LH}	M_W	I_{100}		M_{LH}	M_W	I_{100}
	Kamchatka			03.1964	6.0	6.02	2.0
10.1928	6.1	6.1	5.5	05.1964	6.8	6.6	6.5
11.1929	6.1	6.1	5.5	06.1964	7.2	6.99	6.0
03.1934	6.3	6.23	4.0	03.1966	5.9	5.95	4.5
08.1947	6.2	6.15	5.0	06.1966	6.0	6.02	6.0
11.1952	8.5	9.0	8.35	01.1968	7.2	6.99	5.0
05.1959	7.6	7.44	7.5	02.1968	6.5	6.38	3.5
10.1969	7.7	7.56	6.6	07.1968	6.0	6.02	4.0
12.1971	7.8	7.7	7.0	08.1969	8.2	8.16	7.0
09.1974	5.8	5.89	4.5	08.1971	6.4	6.3	5.0
04.1975	6.0	6.02	3.0	02.1973	7.5	7.32	6.5
04.1975	6.2	6.15	3.0	03.1973	6.3	6.23	4.7
01.1976	6.3	6.23	5.5	04.1973	6.3	6.23	4.5
01.1980	6.1	6.1	3.5	06.1973	7.9	7.8	7.1
01.1980	6.0	6.02	3.5	06.1973	6.5	6.38	5.6
03.1980	5.7	5.7	5.5	06.1973	6.0	6.02	5.0
11.1980	6.8	6.6	4.0	06.1973	6.4	6.3	3.5
01.1983	6.1	6.1	3.0	06.1973	7.4	7.2	7.3
12.1984	7.5	7.32	5.5	06.1973	6.0	6.02	5.0
01.1989	6.4	6.3	3.5	07.1973	6.5	6.38	4.0
05.1989	6.4	6.3	5.0	08.1973	5.8	5.89	4.0
	Kurils			09.1974	7.2	6.99	5.0
03.1952	8.3	8.24	8.0	06.1975	7.2	6.99	5.6
03.1952	6.8	6.6	5.0	06.1975	6.7	6.48	5.5
03.1952	6.5	6.38	5.0	06.1975	7.0	6.78	5.0
03.1952	7.2	6.99	5.8	06.1975	6.7	6.48	3.6
03.1952	5.9	5.95	4.5	01.1976	7.2	6.99	5.5
03.1952	6.0	6.02	3.7	03.1978	7.9	7.8	7.2
04.1952	6.0	6.02	5.0	02.1980	7.2	6.99	6.0
04.1952	6.2	6.15	5.5	02.1980	6.4	6.3	3.5
05.1952	6.5	6.38	4.0	12.1980	6.9	6.69	4.4
07.1952	6.2	6.15	5.5	09.1981	6.7	6.48	6.5
05.1953	6.2	6.15	5.0	11.1981	6.0	6.02	4.0
07.1953	6.9	6.69	5.0	02.1983	6.3	6.23	4.7
10.1953	6.0	6.02	4.8	03.1983	6.1	6.12	4.0
11.1958	8.2	8.16	9.0	04.1983	6.6	6.42	5.7
01.1961	5.9	5.95	4.5	12.1984	6.5	6.38	4.5
02.1961	7.0	6.78	6.0	05.1985	6.7	6.48	5.4
10.1963	8.1	8.1	7.0				

A significant problem was caused by the conversion of M_{LH} magnitude to be found in most catalogs to the moment magnitude M_W, which was preferred for the problem in hand. We used all seismic moment (M_0 or M_W) determinations that could be found in the

literature. In cases where neither was available, M_{LH} was converted to M_W using regional regression curves [6] specially derived for the purpose.

The macroseismic data on Japanese earthquakes were used in the form of a $J(M)$ relation based on them:

$$J_{100} = 1.5M_J - 6.2. \tag{35}$$

The above relation was obtained by Hashida [22], [23] from a large amount of macroseismic data; the intensity J was that on the Japanese 7-grade *JMA* scale, the magnitude being that on the Japanese scale $M_{JMA}(M_J)$. The conversion of *JMA* intensity to the 12-grade *MSK* scale was carried out by directly interpreting the descriptions for each intensity in the *JMA* scale [3] to find the corresponding *MSK* intensities [7]. The following relations were obtained:

Scale	Intensity						
JMA	1	2	3	4	5	6	7
MSK	2	3.8	4.7	6.0	7.0	9.0	(10.5)

The relation can be represented to within satisfactory accuracy as a broken line:

$$I = \begin{cases} 7.1 + 1.2(J-5); & J < 5 \\ 7.1 + 1.9(J-5); & J > 5 \end{cases}. \tag{36}$$

Using (36) and the regression curves connecting M_{LH} and M_J from [6], and we converted the Hashida relation (35) to the M_{LH} and *MSK* scales.

One can see from Fig. 5 that the data points for Kamchatka and the Kurils are in good agreement with the modified Hashida relation for Japan, so that the two regions can be regarded as being of one and the same type.

When observations are compared to the $I_{100}(M_{LH}(M_W))$ relation derived from the macroseismic equation obtained for Kamchatka [13]

$$I = 1.5M_{LH} - 2.63\lg r - 0.0087r + 2.5, \tag{37}$$

it transpires that (37), which is presently in use, is an upper bound on the data points, overestimates the intensity compared with the observations, and has to be replaced.

A new relation to be recommended for use was derived by, first, fitting a linear regression line $I(M_W)$ to the data points in Fig. 5. The result can be written down as follows:

$$I_{100} \pm 0.85 = (1.54 \pm 0.15)M_W + (-5.0 \pm 0.998). \tag{38}$$

This line (marked 4 in Fig. 5) is a moderately satisfactory description of I_{100} data for the Kurils, Kamchatka and Japan. A slightly better fit was obtained with the line that represents the orthogonal regression (marked 3 in Fig. 5)

$$I_{100} \pm 0.87 = (1.77 \pm 0.15)M_W + (-6.5 \pm 1.0). \quad (39)$$

However, the theory developed here enables one to incorporate, not only the far-zone linear relation $I_{100}(M_W)$, but also the trend toward a saturation of I_{100} with a source size of $\geq$ 100 km. A theoretical relation connecting I_{100} and M_W (line 1) was derived assuming $C_M = 1.85$. This value of C_M was found by a trial-and-error method. The vertical level was then fitted by minimizing the mean error. This level was specified by setting $I_{100}(M_W=8) = 7.75$ intensity units. The resulting curve (marked 6 in Fig. 5) is the estimate of $I_{100}(M_W)$ recommended for use.

The next step was to fit the attenuation law $\Phi(r)$. It should be emphasized that the attenuation in the region shows marked lateral variations, so that the result of this part of the present study provides merely a very smoothed picture. It was supposed that the attenuation curve in [13] which had been fitted to observations made in the Kurils and Kamchatka was a good representation of the empirical trend. The shape of the curve was simulated by the simple law (14) where we set $n = 1$ as representing the leading part played by S waves (direct or scattered at small angles). The fit was thus reduced to estimating of r_Q. Figure 6 displays a series of theoretical $I(r)$ curves for $M_W = 8$ and a range of r_Q values. Also shown is the corresponding empirical curve (37) which describes the observations in the distance range 50–500 km. All of these curves have a common point, $I_{100}(M_W=8) = 7.75$ ($I_b = 7.75$ at $M_b = 8$ and $r_b = 100$ km). The value $r_Q = 90$ km emerges as the optimal from comparison of the theoretical curves and the empirical relation. Assuming the characteristic frequency of the acceleration spectrum to be $f_1 = 2$ Hz under these conditions, we arrived at the value $Q = 2\pi f_1 r_Q/c = 280$ with an average crust–mantle velocity of 4 km/s. This value is consistent with the estimates of shear-wave Q in the Kamchatkan lithosphere [17].

Figure 6 also shows theoretical $I(r)$ curves for other values of M_W, a fixed $r_Q = 90$ km, and the same I_b, M_b, and r_b. The resulting family of curves is a graphic picture of how source dimension influences intensity attenuation. The curves for $M_W = 8$, not to speak of $M_W = 9$, flatten out close to the source compared with those for lower magnitudes, thus demonstrating the saturation effect.

DETERMINATION OF THE EMPIRICAL I (M_W, r) RELATION AND THE PARAMETERS OF THE (I–M–r) MODEL FOR CONTINENTAL NORTH EURASIA

The model parameters for continental North Eurasia were determined exactly as was done for the Kamchatka–Kurils–Japan region. Continental North Eurasia contains several continental seismic regions of the former Soviet Union. The first step was to investigate $I(M_W)$ relations at two distances from the source, namely, 30 (I_{30}) and 100 km (I_{100}). The

data to which the relations were to be fitted were taken from [9] and treated as described for the Kamchatka–Kurils–Japan region. The M_{LH}–M_W conversion was based on the nonlinear relations from [6].

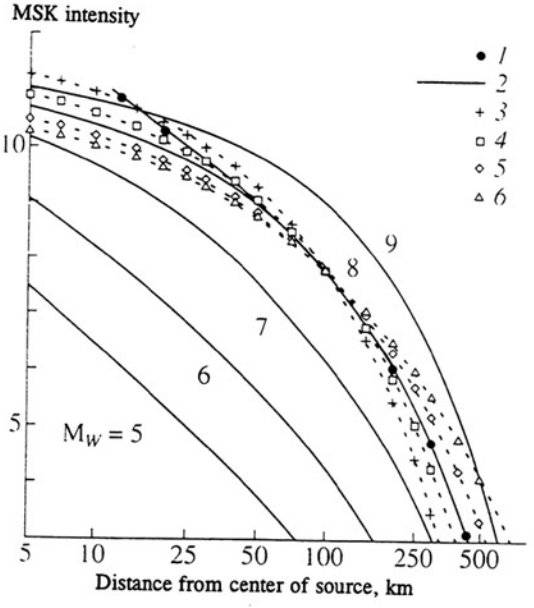

Figure 6 Curves of intensity versus distance for the Kurils–Kamchatka–Japan region: *1* – based on data from [13]; *2* – based on our model with r_Q = 90 km; *3–6* – calculated for this model with M_W = 8 and r_Q equal to 50, 70, 130, and 200 km, respectively.

Figure 7 shows the relations between magnitude M_W and intensity of shaking I_{100} at 100-km distance from the source based on data of 303 earthquakes. The standard (average) $I(M_W)$ relation due to Shebalin [9]

$$I = M_{LH} - 3.5 \lg r + 3.0 \tag{40}$$

(marked 2 in Fig. 7) was found to be in good agreement with the observations (*1* in Fig. 7). Therefore, the standard level for $I(M_W)$ was chosen to be the well documented point corresponding to M_{LH} = 6.0 (M_W = 6.23), r = 50 km, and I_r = 6. The theoretical $I(M_W)$ relation (*5* in Fig. 7) was derived upon the assumption $C_M = dI/dM = 1.85$, similarly to what we did above. The resulting relation was practically identical with the standard Shebalin formula, except for the highest magnitudes. The standard linear regression $I(M_W)$ based on the experimental data points yielded C_M = 1.42. The relevant curve in Fig. 7 (*3*) was a poor fit to the data for higher M_W. The orthogonal $I(M_W)$ regression yielded C_M = 1.68; the relevant straight line in Fig. 7 (*4*) was a good fit in the entire range of M_W and was close enough to the Shebalin curve.

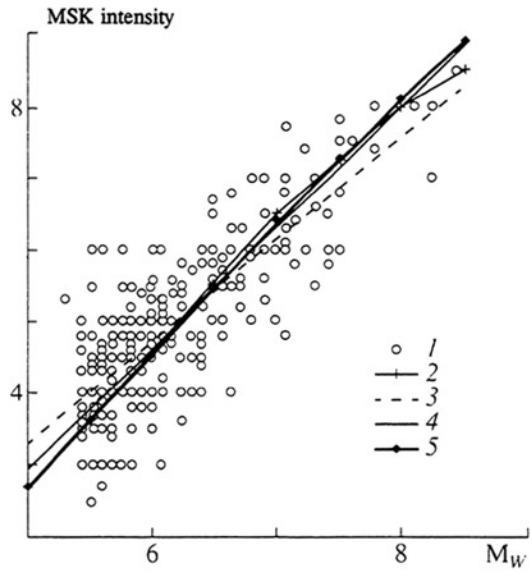

Figure 7 Intensity vs. M_W at 100-km distance for continental North Eurasia: *1* – data points; *2* – Shebalin relation [9]; *3* – linear regression; *4* – orthogonal regression for data points shown; *5* – recommended $I_{100}(M_W)$ relation.

We tried to detect differences in $I_{100}(M_W)$ between individual regions of North Eurasia such as the Caucasus, Kopet Dag, Baikal, etc. We did not succeed in detecting any significant regional differences in the slope or absolute level of the curve based on the available amount of macroseismic data.

Figure 8 presents relations between M_W and intensity of shaking I_{30} at a distance of 30 km from the source based on data of 164 earthquakes. The standard linear regression (*3*) yielded $C_M = 1.63$, but was no good fit either at high M_W. The orthogonal regression (*4*) was a better fit to the data points, the value of C_M being 1.82. The Shebalin relation (*2*) was a satisfactory fit, whereas the line representing the Rautian formula [10] when converted to M_W (*5*) showed a too low slope. The theoretical $I(M_W)$ relation (*6*) with $C_M = 1.85$ yielded the best fit to the data points shown in this plot.

Summing up, the theoretical curve with $C_M = 1.85$ is a good fit to the data for continental North Eurasia at the distances 30 and 100 km, even though it is at variance with the formal standard linear regression line. However, the latter ignores the few data points at high magnitudes by the method it uses data, so that the standard linear regression estimate of C_M can be regarded as the lower bound.

An attempt to specify the attenuation law $\Phi(r)$ using (14) led to an unsatisfactory result: I values were overestimated at large r and high M. The use of (14a) with $n_1 = 1$, $n_2 = 0.5$, and $r_{Q1} = r_{Q2}$, and $r_c = 70$ km fitted the data well. Trying several values of

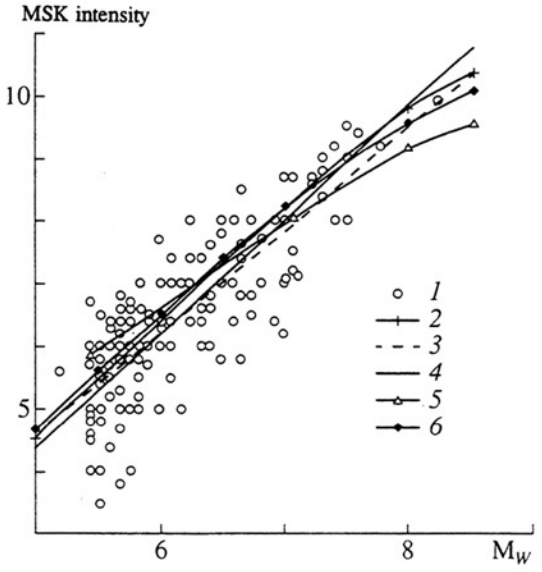

Figure 8 Intensity vs. M_W at 30-km distance for continental North Eurasia: *1* – data points; *2* – Shebalin relation [9]; *3* – linear regression; *4* – orthogonal regression for data points shown; *5* – recommended $I_{100}(M_W)$ relation.

r_Q, we preferred r_Q = 100 km (Fig. 9). Corresponding to it is Q = 314 for the selected characteristic frequency 2 Hz. An internal control on the method was possible thanks to the availability of independent observations at distances 30 and 100 km. As pointed out above, the slopes in the intensity-magnitude relation were consistent, and so were the absolute levels of the relations.

Figure 9 presents theoretical $I(r)$ curves for M_W = 5–8, as well as empirical curves obtained by Shebalin's formula. The theoretical and empirical curves are in satisfactory agreement, except at short and large distances for high M_W. The Shebalin formula is grossly inadequate at short distances by overestimating the effect, because it disregards the source dimension, while at large distances it errs by inaccurate incorporation of path attenuation. The model curves clearly take the source extent into account: those for $M_W \geq 8$ are flattening close to the source compared to the curves for lower magnitudes.

DISCUSSION OF RESULTS

It is an urgent problem to deduce macroseismic patterns by using the wave theory for incoherent radiators. The first attempt at doing so described above was a success. The parameters in (32) for two regions were determined.

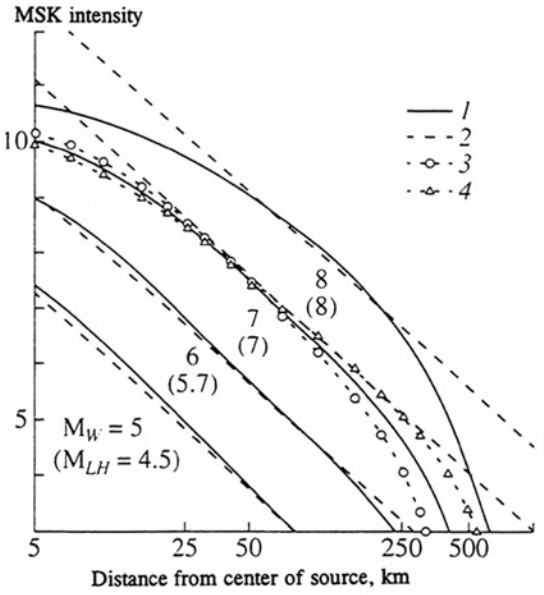

Figure 9 Intensity vs. distance for continental North Eurasia: *1* – our model with $r_Q = 100$; *2* – Shebalin relation [9]; *3*, *4* – calculated for our model with $M_W = 7$ and r_Q equal to 70 and 150 km, respectively.

Kamchatka–Kurils–Japan: $C_A = 1.667$, $C_M = 1.85$, $n = 1$, $r_Q = 90$ km, $I_b = I(M_b = 8, r_b = 100 \text{ km}) = 7.75$ intensity units, $C_{MS} = 4.1$.

Continental North Eurasia: $C_A = 1.667$, $C_M = 1.85$, $n_1 = 1$, $n_2 = 0.5$, $r_{Q1} = r_{Q2} = 100$ km, $r_c = 70$ km, $I_b = I(M_{LHb} = 6\ (M_W = 6.23); r_b = 50 \text{ km}) = 6.0$ intensity units, $C_{MS} = 4.1$.

The models were tested for correctness and found to be adequate, namely: the $I(M_W)$ relation at $r_b = 100$ km was close to linear; the slope of the line was 1.85, therefore, as expected (see our comment on (22)) was slightly higher than 1.667, the latter value being relevant to a spectral ω^{-2}-model; the $I(r)$ relation was consistent with the hypothesis of short-period energy generated by a point source propagating as *S* waves in a homogeneous earth with $Q \sim 300$ at 2 Hz.

Remarkably enough, the values of Q for these two major regions were satisfactorily similar, the regions being essentially different as to geometrical spreading. It should be noted that the estimates of Q derived from macroseismic data were meaningful enough. These estimates relied on the attenuation of (spectral) power rather than of peak amplitudes, hence were fairly well consistent with determinations of Q, this parameter relying precisely on energy attenuation. It is appropriate to say that the propagation of

seismic waves over regional distances involves lengthening of wave trains with increasing distance due to scattering and dispersion. Hence the difference between the attenuation laws for peak amplitudes and spectra: increasing record duration an extra factor to reduce the peak amplitude.

CONCLUSION

We represented the earthquake source as an incoherent radiator which has a constant (over the source plane area) density of seismic energy combined with the relation of intensity to ground motion parameters using the approach of F. F. Aptikaev and N. V. Shebalin. This enabled us to model the basic macroseismic relation (I–M–r) successfully for specific regions, namely, Kamchatka–Kurils–Japan and continental North Eurasia.

One important advantage of this approach is the automatic incorporation of three nonlinearities which tend to distort interpretations of macroseismic data when treated by conventional techniques: (1) saturation of intensity close to the source; (2) nonlinear $I(\lg a)$ relation; and (3) magnitude saturation at high M_0.

The simplicity of the scheme of calculation suggested here enables it to be included, instead of formulas for the calculation of $I(M, r)$, into algorithms needed for seismic zonation and seismic risk assessment. This procedure removes the problem of overestimated intensity at short distances and automatically models the ellipticity of isoseismals due to the source extent.

Our I–M–r model was used for making a new seismic zonation map of North Eurasia [11], [12]: the map for the Russian Federation (GSZ-97) was adopted as the basis for a new version of the Construction Norms and Specifications (CNiP–P–7 as abbreviated in Russian).

This work was supported by the Russian Foundation for Basic Research, project 97-05-65056.

REFERENCES

1. F. F. Aptikaev, in: *The Intensity Scale and Methods for Measuring Earthquake Intensity* (in Russian) (Moscow: Nauka, 1975): 234–239.
2. F. F. Aptikaev and N. V. Shebalin, in: *Studies in Earthquake Hazard* (in Russian) (Moscow: Nauka, 1988): 98–107.
3. B. A. Bolt, W. L. Horn, G. A. Macdonald, and R. F. Scott, *Geological Hazards* (Berlin–Heidelberg–New York: Springer–Verlag, 1977).
4. A. A. Gusev, *Vulkanol. Seismol.* **6**, N1: 3–22 (1984).
5. A. A. Gusev, *Vulkanol. Seismol.* **10**, N1: 41–55 (1988).
6. A. A. Gusev and V. N. Melnikova, *Volcanol. Seismol.* **12**, N6: 723–733 (1990).

7. I. A. Ershov and N. V. Shebalin, in: *Prediction of Earthquake Hazard* (in Russian) (Moscow: Nauka, 1984): 78–89.
8. S. V. Medvedev, *Engineering Seismology* (in Russian) (Moscow: Stroiizdat, 1962).
9. *A New Catalog of Large Earthquakes in the USSR Area Since the Earliest Times Until 1975* (in Russian) (Moscow: Nauka, 1977).
10. T. G. Rautian, V. I. Khalturin, and N. T. Dotsev, *Voprosy Inzhenernoi Seismologii* **30**: 98–109 (1989).
11. V. N. Strakhov, V. I. Ulomov, and L. S. Shumilina, *Fizika Zemli* N10: 92–96 (1998).
12. V. I. Ulomov and L. S. Shumilina, *Seismostoikoe Stroitelstvo* N4: 30–34 (1998).
13. S. A. Fedotov and L. S. Shumilina, *Izv. AN SSSR. Fizika Zemli* N9: 3–16 (1971).
14. Yu. K. Chernov, in: *Macroseismic and Instrumental Studies of Large Earthquakes* (in Russian) (Moscow: Nauka, 1985): 150–158.
15. N. V. Shebalin, in: *Seismic Zonation of the USSR* (in Russian) (Moscow: Nauka, 1968): 95–111.
16. N. V. Shebalin, in: *The Intensity Scale and Methods for Measuring Earthquake Intensity* (in Russian) (Moscow: Nauka, 1975): 222–233.
17. I. R. Abubakirov and A. A. Gusev, *Phys. Earth Planet. Inter.* **64**: 52–67 (1990).
18. K. Aki, *J. Geophys. Res.* **72**: 1217–1231 (1967).
19. A. Arias, in: *Seismic Design for Nuclear Power Plants* (Cambridge a.o.: M.I.T. Press, 1970): 438–483.
20. B. Gutenberg and C. F. Richter, *Bull. Seismol. Soc. Amer.* **32**, N3: 163–191 (1942).
21. J. F. Evernden, *Bull. Seismol. Soc. Amer.* **65**: 1287–1315 (1975).
22. T. Hashida, *Bull. Earthq. Res. Inst.* **62**: 247–287 (1987).
23. T. Hashida and K. Shimazaki, *J. Phys. Earth* **35**: 367–379 (1987).
24. G. W. Housner, *Bull. Seismol. Soc. Amer.* **45**: 197–218 (1955).
25. K. Kanai, *Bull. Earthq. Res. Inst.* **21**, Pt. 2: 393–401 (1951).
26. H. Kanamori and D. L. Anderson, *Bull. Seismol. Soc. Amer.* **65**: 1073–1095 (1975).